CHIN. PHYS. LETT. Vol. 27, No. 1 (2010) 016401

A Thermodynamic Cavitation Model for Cavitating Flow Simulation in a Wide Range of Water Temperatures *

ZHANG Yao(张瑶), LUO Xian-Wu(罗先武)**, JI Bin(季斌), LIU Shu-Hong(刘树红), WU Yu-Lin(吴玉林), XU Hong-Yuan(许洪元)

State Key Laboratory for Hydroscience and Engineering, Tsinghua University, Beijing 100084

(Received 16 January 2009)

A thermodynamic cavitation model is developed to simulate the cavitating water flow in a wide temperature range. The thermal effect on bubble growth during cavitation is introduced in the developed model by considering both pressure difference and heat transfer between the vapor and liquid phase. The cavitating turbulent flow over a NACA0015 hydrofoil has been simulated at various temperatures from room temperature to 150°C by using the present cavitation model, which has been validated by the experimental data. It is seen that the thermodynamic effects of cavitation, vapor depression and temperature depression are much more predominant in high temperature water compared with those in room temperature water. These results indicate that the proposed thermodynamic cavitation model is reasonably applicable to the cavitating water flow in a wide temperature range.

PACS: 64. 70. Fm, 47. 55. Ca DOI: 10.1088/0256-307X/27/1/016401

Since most of the cavitation phenomena have been treated in water flows of room temperature, it is usually assumed that the cavitation process is adiabatic. However, there are cases to transport high temperature water and cryogenic liquid as working media by a turbo-pump. The cavitation behavior in these cases must be quite different from that in room temperature water, since it is reported that the suction performance of turbo-pump for high temperature water was improved as compared with that of room temperature.[1] This favorable feature is interpreted as the thermodynamic effect of cavitation. In general, the vapor bubble absorbs the latent heat of vaporization from the bulk liquid when cavitation occurs. The vaporization results in a temperature depression in the vicinity of the liquid-vapor interface. Thus, the process of cavitation in the flows of high temperature water and/or cryogenic fluids will be managed by the thermodynamic effects.[2]

To predict the thermodynamic effects of cavitation, many studies have been conducted. Stahl and Stepanoff[3] estimated the head depression due to the thermodynamic effect by using the so-called "B-factor" method for turbo-pumps. Another similar semi-empirical procedure, i.e., the entrainment theory, was proposed by Holl *et al.*[4] In recent years, numerical modeling for thermodynamic effects of cavitation have been attempted based on homogeneous methods such as the bubble two-phase flow (BTF) model and the transfer equation model (TEM).[5–8] Such numerical simulation of cavitating flow is desirable to understand the related phenomena in detail.

Among those cavitation models, however, the pressure difference between the vapor and liquid phase is the only dominant factor for controlling the bubble growth, and the thermal effect due to the fact that the heat transfer between the vapor and liquid phase has not been taken into account in the process of bubble growth. Since the temperature depression in the vicinity of the liquid-vapor interface may have considerable influence on the bubble growth, it is expected to include the effect of heat transfer in a cavitation model. Consequently, a new thermodynamic cavitation model that accounts for the thermal effects of cavitation has been developed.

In this Letter, a homogeneous liquid-gas mixture model is assumed to simulate the cavitating flow in a wide range of water temperature, i.e., from room temperature to 150°C. The governing equations, i.e. the incompressible continuity equation, the momentum equation or the Navier–Stokes equation, and the energy equation, for solving the cavitating flow are as follows:

$$\frac{\partial \rho_m}{\partial t} + \nabla \cdot (\rho_m \boldsymbol{U}) = 0, \tag{1}$$

$$\frac{\partial}{\partial t}(\rho_m \boldsymbol{U}) + \nabla \cdot [\rho_m \boldsymbol{U} \times \boldsymbol{U} - \mu_m(\nabla \boldsymbol{U} + (\nabla \boldsymbol{U})^T)] = -\nabla p, \tag{2}$$

$$\frac{\partial}{\partial t}(\rho_m h_m) + \nabla \cdot (\rho_m h_m \boldsymbol{U} - \lambda_m \nabla T_m) = (\dot{m}^+ - \dot{m}^-) h_{fg}, \tag{3}$$

where ρ, μ, and λ are the density, molecular viscosity and thermal conductivity; U, p, h, and T are the velocity, static pressure, enthalpy and the temperature at a local point of cavitating flow field; h_{fg} is latent heat; subscripts l, v, and m denote the liquid phase, vapor phase and the mixture; $\dot{m}^+$ and $\dot{m}^-$ are the condensation rate and the vaporization rate.

In Eq. (3), the source term $(\dot{m}^+ - \dot{m}^-)h_{fg}$ represents the heat transfer caused by mass transfer between the vapor phase and liquid phase.

The liquid volume fraction α_l is governed by the

*Supported by the National Natural Science Foundation of China under Grant Nos 50676044 and 10532010, and Beijing Natural Science Foundation under Grant No 3072008.

**Email: luoxw@tsinghua.edu.cn

© 2010 Chinese Physical Society and IOP Publishing Ltd

transport equation

$$\frac{\partial}{\partial t}(\alpha_l \rho_l) + \nabla \cdot (\alpha_l \rho_l \boldsymbol{U}_l) = \dot{m}^+ - \dot{m}^-. \tag{4}$$

Thus, for the mixture, $\rho_m = \rho_v \alpha_v + \rho_l \alpha_l$, $\mu_m = \mu_v \alpha_v + \mu_l \alpha_l$, where α_v is the vapor volume fraction.

So far, many cavitation models based on the transport equation have been derived from the Rayleigh–Plesset equation[9] which describes the growth of a gas bubble in liquid. By neglecting the second order terms and the surface tension, the Rayleigh–Plesset equation can be simplified to

$$\frac{dR_b}{dt} = \sqrt{\frac{2}{3}\frac{p_v - p}{\rho_l}}, \tag{5}$$

where R_b is the bubble radius, p_v is the pressure in the bubble, alternatively saturated vapor pressure, p is the static pressure in the liquid surrounding the bubble.

It is noted that in most of the TEM based cavitation models, mass transfer is mainly enhanced by the mechanical effects, namely the pressure difference between the liquid phase and vapor phase, rather than the thermal effects. The cavitation model adopted by the commercial code ANSYS-CFX v11,[10] which uses the condensation rate and vaporization rate as shown in Eqs. (6) and (7), respectively, is a typical example of those kinds of cavitation model,

$$\dot{m}^+ = C'_{\rm con} \frac{3\alpha_v \rho_v}{R_b} \sqrt{\frac{2}{3}\frac{(p - p_v)}{\rho_l}}, \tag{6}$$

$$\dot{m}^- = C'_{\rm vap} \frac{3 r_g (1 - \alpha_v) \rho_v}{R_b} \sqrt{\frac{2}{3}\frac{(p_v - p)}{\rho_l}}, \tag{7}$$

where $C'_{\rm con}$ and $C'_{\rm vap}$ are the empirical parameters for condensation and vaporization rate, r_g is the volume fraction of the nucleation sites in the bulk liquid.

For the case of cavitation in water at high temperatures, the phase change due to the thermal effect should also be taken into account. Based on the studies of boiling heat transfer, the process of vapor bubble growth can be divided into two stages.[11] First, the vapor generation which can be described by the bubble dynamics is mainly controlled by the pressure difference between liquid phase and vapor phase. Once the bubble generation is developed, the further bubble growth will depend on the heat transfer from superheated liquid to the liquid-vapor interface. The bubble growth during this second stage[12] is defined by

$$R_b = 2 C_s \sqrt{a_l t}, \tag{8}$$

where C_s and a_l are the empirical coefficient and the liquid thermal diffusivity.

Figure 1 shows the above-mentioned concept of the cavitation process considering the thermal effects. The distribution of temperature and pressure in the central bubble is assumed to be uniform. The pressure in the bubble equals to the saturated pressure p_v and the temperature equals to the saturated temperature T_s. There is a thermal boundary between the bubble and bulk liquid. The temperature difference between the outer and inner side of the thermal boundary is expressed as $\Delta T = T - T_s$, and ΔT denotes the temperature depression.

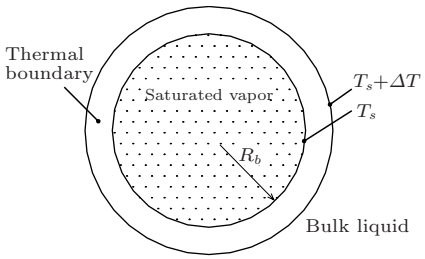


Fig. 1. Concept of thermal boundary.

In the present cavitation model, the equation developed by Plesset and Zwick[13] is adopted so as to take the effect of temperature depression on bubble growth into consideration. Then, the empirical coefficient in Eq. (8), C_s, can be written as

$$C_s = \sqrt{\frac{3}{\pi}}\frac{\rho_l C_p \Delta T}{\rho_v h_{fg}}. \tag{9}$$

Thus, the equation for the bubble growth by heat transfer will be given in the form

$$\frac{dR_b}{dt} = \sqrt{\frac{3}{\pi}}\frac{\rho_l C_p \Delta T}{\rho_v h_{fg}}\sqrt{\frac{a_l}{t}}. \tag{10}$$

By combining Eqs. (5) and (10), the condensation rate and vaporization rate for the proposed cavitation model are expressed as, respectively,

$$\dot{m}^+ = C_{\rm con}\frac{3\alpha_v \rho_v}{R_b}\left(\sqrt{\frac{2}{3}\frac{(p - p_v)}{\rho_l}} + \sqrt{\frac{3}{\pi}}\frac{\rho_l C_p (T_s - T)}{\rho_v h_{fg}}\sqrt{\frac{a_l}{t}}\right), \tag{11}$$

$$\dot{m}^- = C_{\rm vap}\frac{3 r_g (1 - \alpha_v) \rho_v}{R_b}\left(\sqrt{\frac{2}{3}\frac{(p_v - p)}{\rho_l}} + \sqrt{\frac{3}{\pi}}\frac{\rho_l C_p (T - T_s)}{\rho_v h_{fg}}\sqrt{\frac{a_l}{t}}\right), \tag{12}$$

where $C_{\rm con}$ and $C_{\rm vap}$ are the empirical parameters for condensation and vaporization rate. Their values are 0.002 and 10, respectively, based on the calibration.

It is noted that Eqs. (10), (11) and (12) are time-dependent. Since the bubble growth is mainly controlled by ΔT during the second stage of the cavitation process, the variable t in those equations can be replaced by a constant value which represents the bubble growth time for better calculation convergence in this study.

In order to make an accurate prediction of cavitating turbulent flow, the proposed cavitation model (Eqs. (11) and (12)) is combined with the governing equations (1)–(3). Further, the thermodynamic properties of liquid and vapor such as density, saturated pressure, etc., are also defined as functions of temperature and pressure at the local point of flow field accordingly. As the three-dimensional turbulent flow is treated, the standard $k-\varepsilon$ turbulence model is used.

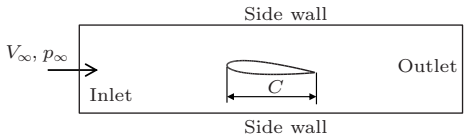


Fig. 2. Computational domain for cavitating flow around the NACA0015 hydrofoil.

In order to evaluate the proposed thermodynamic cavitation model, the steady cavitating water flow around hydrofoil NACA0015 is simulated. The hydrofoil has dimensions of 115 mm(chord length)×80 mm(span length). The computational domain, which corresponds to the experimental setup,[14] is schematically shown in Fig. 2. In the computational domain, the unstructured mesh was generated, and the grid near the foil surface was refined. Boundary conditions are as follows: uniform velocity, temperature and turbulence intensity for the inflow plane, the averaged static pressure for the outflow plane, and non-slip condition for the walls including the foil surface as well as both sides of the domain. The calculation conditions are: the attack angle of 5 degree, the inlet velocity of 8 m/s and the cavitation number σ $\left(=\frac{p_\infty - p_v}{0.5\rho_l u_\infty^2}\right.$, p_∞ and u_∞ are the static pressure and velocity at the inflow plane$\left.\right)$ of 1.5. Four kinds of water temperature are used, i.e., 25°C (equivalent to the room temperature), 50°C, 100°C, and 150°C. Its effect on the cavitating flow around the foil is studied numerically.

From Figs. 3–8, the calculated results on the central plane in the span-wise direction of the domain are shown. Illustrations in Fig. 3 show the contour maps of the calculated vapor volume fraction at different temperature in water. It is seen that (1) if the temperature varies from 25°C to 50°C, though the cavity length seems to become slightly longer, the vapor concentration in the cavity is obviously decreased; (2) above 50°C, the cavity size decreases with the increasing temperatures; (3) disappearance of the cavity zone from the foil surface is calculated when the water temperature is 150°C. The result indicates that the vapor depression can be predicted fairly well.

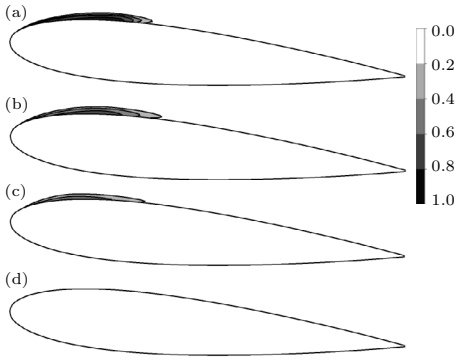


Fig. 3. Vapor volume fraction along the foil surface: (a) $T = 25$°C, (b) $T = 50$°C, (c) $T = 100$°C, and (d) $T = 150$°C.

In Figs. 4 and 5, the distribution of the pressure coefficient $-C_p$ $\left(=\frac{p_\infty - p}{0.5\rho_l u_\infty^2}\right)$ along the foil surface is shown. The legend of the horizontal axis in the figures, x/C (C denotes the chord length of the foil), is the relative coordinate along the inflow direction. From them, good agreement between the numerical results and the experimental data is observed in both the cases.

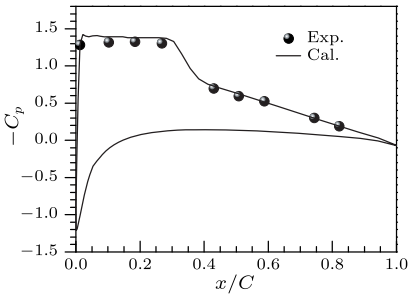


Fig. 4. Pressure coefficient along the foil surface at water temperature of 25°C.

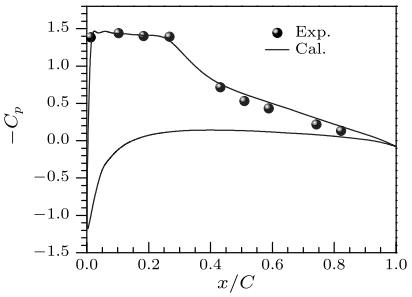


Fig. 5. Pressure coefficient along the foil surface at water temperature of 50°C.

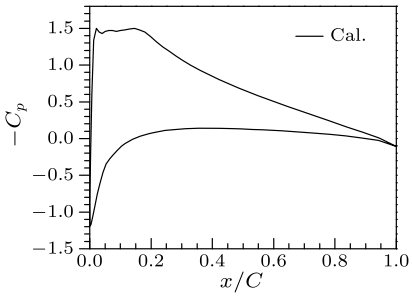


Fig. 6. Pressure coefficient along the foil surface at water temperature of 100°C.

Figures 6 and 7 also show the distribution of $-C_p$ along the foil surface at high temperatures of 100°C and 150°C. It is seen in these figures that the cavitation is suppressed with the increasing water temperature. This will be a typical feature of the thermodynamic effect of cavitation. Moreover, it seems that the decrease of cavity length accelerates at high temperature level such as the temperature changing from 100°C to 150°C. Compared to the case at room temperature ($T = 25$°C) shown in Figs. 3(a) and 4, the cavity size at 50°C shown in Fig. 3(b) decreases slightly. If the temperature increases to 100°C, it is seen that the cavity size shown in Fig. 3(c) becomes much smaller and the cavity length estimated from

Fig. 6 is shortened by about 45%. At the temperature of 150°C, the cavity almost disappears as shown in Fig. 3(d), and the cavity length in Fig. 7 is dramatically depressed (shortened by 87%).

The reason for the vapor depression must be related to the thermal properties of the water at different temperature levels. The key point is that the vaporization is dramatically reduced due to the much steeper slope of vapor pressure-temperature curve, i.e., the $p_v - T$ curve,[2] at high temperature. At the temperatures of 25°C, 50°C, 100°C and 150°C, slope of the $p_v - T$ curve is approximately 166 Pa/K, 551 Pa/K, 3354 Pa/K and 12104 Pa/K, respectively. In other words, the slope at 150°C is 3.6 times as large as that at 100°C, 22 times at 50°C, and 73 times at 25°C. As a result, much larger decrease of vapor saturated pressure for higher temperature water occurs, and the vaporization rate decreases according to Eq. (12). Consequently, the growth of vapor is suppressed due to the considerable decrease of p_v, which is regarded as the thermodynamic effect.

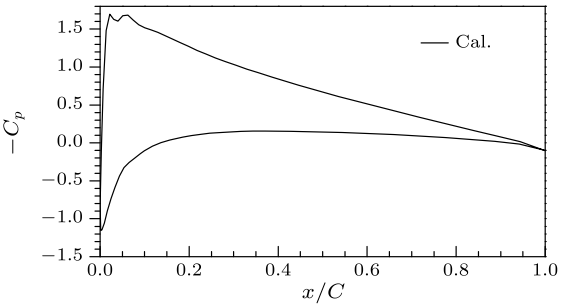


Fig. 7. Pressure coefficient along the foil surface at water temperature of 150°C.

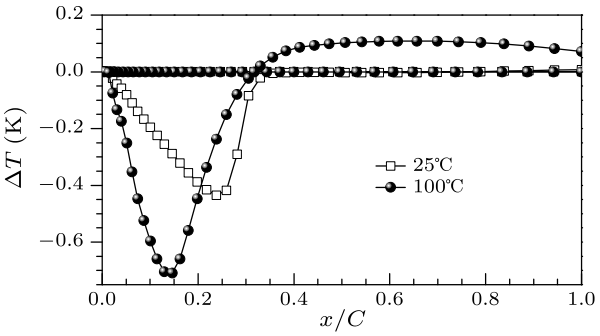


Fig. 8. Variation of temperature differential along the foil surface.

Another evidence of the thermodynamic effects is the temperature depression during cavitation. As a typical example, Fig. 8 shows the variation of temperature difference between the bulk liquid and vapor along the foil surface at temperatures of 25°C and 100°C. It is noted that the maximum temperature depression at 25°C is near 0.45 K, while that at 100°C is near 0.75 K. The difference of temperature depression is resulted from the different liquid-vapor density ratios for the water at each temperature. The vapor-liquid density ratio at 25°C is 0.231×10^{-4}, much less than that at 100°C, i.e., 6.23×10^{-4}. This indicates that much greater mass transfer is necessary for high temperature water to sustain an equal size cavity. As a result, in the case of high temperature water, the liquid in the vicinity of liquid-vapor interface undergoes significant evaporative cooling. Further, the vapor saturated pressure of high temperature water is much more sensitive to the temperature change due to the steep slope of the $p_v - T$ curve. Thus, the temperature depression for high temperature water is larger than that for room temperature water.

It should also be noted that the mixture temperature at the trailing edge of the hydrofoil rises about 0.1 K in the case at temperature of 100°C as shown in Fig. 8. This temperature rise can be interpreted by the heat release when the bubbles collapse at the downstream of the cavity zone along the hydrofoil. Since the evaporative cooling effect is much more significant in water at temperature of 100°C, the heat release will be much intensive than that at the room temperature. Thus, the temperature rise in the high temperature water can be recognized clearly at the downstream of the cavity zone, while that in the room temperature water is negligible.

In summary, a thermodynamic cavitation model is developed in this study to simulate cavitating turbulent flow in a wide range of water temperatures with high accuracy. In the proposed cavitation model, the thermal effect on bubble growth is introduced based on the concept of heat transfer between the vapor and liquid phase. Validation of the developed model is successfully performed from the investigation of the cavitating flow over an NACA0015 hydrofoil for four kinds of water temperatures. Further, the numerical results for water flows at high temperatures of 100°C and 150°C show that there may be a remarkable vapor depression as well as temperature depression in the cavity zone. Consequently, the proposed thermodynamic cavitation model is applicable to simulate the cavitating flow in a wide range of water temperatures.

References

[1] Brennen C E 1994 *Hydrodynamics of Pumps* (London: Concepts NREC and Oxford University) p 142
[2] Deshpande M et al 1997 *J. Fluids. Eng.* **119** 420
[3] Stahl H A and Stepanoff A J 1956 *J. Basic. Eng.* **78** 1691
[4] Holl J W et al 1975 *J. Fluids. Eng.* **97** 507
[5] Tani N and Nagashima T 2002 4th *Int. Conference on Launcher Technology* (Liege, Belgium)
[6] Rapposelli E and Agostino L D 2003 5th *Int. Symposium on Cavitation* (Osaka, Japan)
[7] Utturkar Y, Thakur S and Shyy W 2005 *43rd AIAA Aerospace Sciences Meeting and Exhibit* (Reno, Nevada)
[8] Hosangadi A, Ahuja V and Ungewitter R J 2007 *J. Propulsion. Power.* **23** 1225
[9] Kubota A et al 1992 *J. Fluid. Mech.* **240** 59
[10] ANSYS Inc 2006 *ANSYS CFX-Solver Theory Guide* p 178
[11] Xu J J and Jia D N 2000 *Boiling Heat and Gas-liquid Two Phase Flow* (Beijing: Atomic Energy Press) p 223 (in Chinese)
[12] Yang C X et al 1999 *J. Thermal. Power. Eng.* **14** 246
[13] Plesskt M S and Zwick S A 1954 *J. Appl. Phys.* **25** 493
[14] Cervone A et al 2006 *J. Fluids. Eng.* **128** 326